



## ISTITUTO NAZIONALE DI RICERCA METROLOGICA Repository Istituzionale

Direct quantification of sulfur dioxide in wine by Surface Enhanced Raman Spectroscopy

This is the author's accepted version of the contribution published as:

*Original*

Direct quantification of sulfur dioxide in wine by Surface Enhanced Raman Spectroscopy / Mandrile, Luisa; Cagnasso, Iris; Berta, Ludovico; Giovannozzi, Andrea M; Petrozziello, Maurizio; Pellegrino, Francesco; Asproudi, Andriani; Durbiano, Francesca; Rossi, Andrea M. - In: FOOD CHEMISTRY. - ISSN 0308-8146. - 326:(2020), p. 127009. [10.1016/j.foodchem.2020.127009]

*Availability:*

This version is available at: 11696/65174 since: 2025-02-14T15:49:49Z

*Publisher:*

ELSEVIER SCI LTD

*Published*

DOI:10.1016/j.foodchem.2020.127009

*Terms of use:*

This article is made available under terms and conditions as specified in the corresponding bibliographic description in the repository

*Publisher copyright*

(Article begins on next page)

# Direct quantification of sulfur dioxide in wine by Surface Enhanced Raman Spectroscopy

Luisa Mandrile\*<sup>1</sup>, Iris Cagnasso<sup>1,2</sup>, Ludovico Berta<sup>3</sup>, Andrea M. Giovannozzi<sup>1</sup>, Maurizio Petrozziello<sup>4</sup>,  
Francesco Pellegrino<sup>5</sup>, Andriani Asproudi<sup>4</sup>, Francesca Durbiano<sup>1</sup>, Andrea M. Rossi\*<sup>1</sup>

<sup>1</sup>*Istituto Nazionale di Ricerca Metrologica, Strada delle Cacce 91, 10135 Torino, Italy*

<sup>2</sup>*Department of Applied Science and Technology, Politecnico di Torino, Corso Duca Degli Abruzzi 24, 10129 Torino, Italy*

<sup>3</sup>*Department of Agricultural, Forestry, and Food Sciences (DISAFA), University of Turin, Largo Paolo Braccini 2, 10095 Grugliasco (TO), Italy*

<sup>4</sup>*Centro di ricerca per l'enologia (CREA-ENO), Via Pietro Micca 35, 14100 Asti, Italy*

<sup>5</sup>*Department of Chemistry and NIS Inter-Departmental Centre, University of Torino, Torino, 10125, Italy*

\*Corresponding authors: Luisa Mandrile, tel +39 011 39193344; e-mail [L.mandrile@inrim.it](mailto:L.mandrile@inrim.it) Andrea Mario

Rossi, tel +39 011 3919342 email [a.rossi@inrim.it](mailto:a.rossi@inrim.it)

**Keywords:** sulfur dioxide; wine; Surface Enhanced Raman Spectroscopy, Silver nanoparticles; Measurement comparison.

## Abstract

A rapid Surface Enhanced Raman Spectroscopy (SERS) method to detect SO<sub>2</sub> in wine is presented, exploiting the preferential binding of silver nanoparticles (AgNPs) with sulfur-containing species. This interaction promotes the agglomeration of the AgNPs and inducing the formation of SERS “hot spots” responsible for SO<sub>2</sub> signals enhancement. For increasing SO<sub>2</sub> concentrations from 0 to 100 mg/l in wine simulant, SERS intensity showed an increasing trend, following a Langmuir absorption function ( $R^2 = 0.94$ ). Due to the wine matrix variability, a standard additions method was then employed for quantitative analysis in red and white wines. This method does not require the SO<sub>2</sub> separation but only a matrix pre-cleaning by solid phase extraction. The limit of detection (LOD) was defined for each wine tested, ranging from 0.6 mg/l to 9.6 mg/l. The results obtained were validated

by comparison with the International Organization of Vine and Wine method (OIV-MA-AS323-04A).

## Introduction

Sulfur-containing compounds are widely used as preservatives and antioxidants in foods and beverages, especially in wine (P. Ribéreau-Gayon, D. Dubordieu, B. Donèche, 2007). Sulfites are generally adjusted during wine-making, paying attention to the pH and the type of wine to preserve the quality of the product over storage. In wine-making, sulfites are commonly added either as potassium or sodium metabisulfite which form pH-dependent speciation in solution. Even though they are common and accepted additives in wine, sulfites are classified as allergens provoking the appearance of bronchial spasms, hives and bronchoconstriction in hypersensitive individuals (Gastaminza et al., 1995). For this reason, the level of SO<sub>2</sub> has to be monitored and regulated in final wine products. The Regulation (EU) N° 606/2009 sets legal limits for total SO<sub>2</sub> at 150 mg/l in red wines and 200 mg/l in white wines.

The internationally recognized methods for the combined SO<sub>2</sub> and total SO<sub>2</sub> determination in wine are the Monier-Williams method (OIV-MA-AS323-04A) which consists of an extraction in vapour phase of SO<sub>2</sub> from wine samples and a subsequent acid-base titration. Another established method is the iodometric Ripper method (OIV-MA-AS323-04B) which is, although, highly affected by the matrix and presents repeatability problems. Other techniques were recently proposed as interesting alternatives to the official methods which include: colourimetric (Monro et al., 2012; Oliveira et al., 2009, Prieto et al., 1994; Segundo and Rangel, 2001), electrochemical (Azevedo et al., 1999; Cardwell et al., 1991), chemiluminescence (Huang, Zhang, Zhang, & Zhang, 1999), chromatographic (Koch, Koeppen, Siegel, Witt, & Nehls, 2010), fluorometric (Yang, Guo, & Zhao, 2002) and enzymatic (Smith, 1987) methods. These methods can actually provide a quantitative determination of SO<sub>2</sub> in wine down to the EU limits, but many of them suffer from disadvantages such as time-consuming extraction steps, low accuracy and reproducibility. Therefore, the development of more rapid methods for SO<sub>2</sub> quantification in wine with minimal pretreatment is still required.

In recent years, vibrational spectroscopy techniques found numerous applications in food and beverages analysis as simple, rapid and non-destructive methods (Li-Chan, Chalmers, & Griffiths, 2010). In particular, Raman spectroscopy allows fast detection times, high selectivity due to the Raman fingerprint of molecules and none or minimal preliminary treatment of the sample, since it does not suffer the interference of water. Moreover, the sensitivity of the Raman technique can be increased by several orders of magnitude by Surface Enhanced Raman Spectroscopy (SERS) due to the enhancement of the Raman scattering of molecules adsorbed onto, or in proximity of, a suitable plasmonically active surface, such as roughened nanostructured metal surface, or metal colloids (Dalla Marta et al., 2017, Schluecker, 2014; Virga et al., 2012; Vo-Dinh, 1998). SERS represents a good candidate in food control analysis thanks to the combination of high sensitivity and specificity (Craig, Franca, & Irudayaraj, 2013). Different SERS approaches were already reported for the detection of various food contaminants and additives in food matrices (Mandrile et al., 2018; Pang et al., 2016).

Two recent examples of SERS determination of SO<sub>2</sub> in wine are present in literature (Chen et al., 2016; Deng et al., 2015). They used AuNPs spread on sea urchin-like ZnO nanowires substrates to enhance the signals of sulfites absorbed onto the ZnO nanostructures. A SO<sub>2</sub> quantification in the range between 5 and 300 mg/l and a limit of detection (LOD) of 2 mg/l were obtained. Even though SERS substrates demonstrated an adequate sensitivity in the detection of chemical contaminants, they usually suffer a lack of reproducibility when spot-to-spot tests are compared (Cara et al., 2018; Liu et al., 2014). Therefore, SERS procedures with a good compromise between sensitivity and reproducibility of analysis are still under study to provide reliable results. Conversely to the solid SERS-substrates previously discussed, here a method for the quantification of the SO<sub>2</sub> directly in liquid is proposed, which does not require SO<sub>2</sub> extraction from the wine matrix. The main advantage of the *in liquid* SERS technique is the homogeneity of the liquid samples, which represents a suitable condition to improve the repeatability of SERS measurements (Giovannozzi et al., 2014). In this study, the sample was pre-cleaned using solid-phase extraction (SPE) cartridges to avoid matrix interference and mixed with a suspension of SERS active AgNPs to exploit their interaction with sulfur-containing species. Three spheroidal AgNPs colloids with different nominal diameters, i.e. 4 nm, 30 nm and 55 nm, were tested in EtOH/H<sub>2</sub>O environment for the SERS determination of SO<sub>2</sub>. AgNPs with a diameter of 4 nm were selected as optimal SERS substrate for this application and their specific interaction with SO<sub>2</sub> was studied in wine simulant. The best measurement conditions were evaluated and a SO<sub>2</sub> quantification method for both red and white wines, based on the standard addition strategy, was set-up and validated. The results obtained by in liquid SERS measurements were compared with the results of the official OIV-MA-AS323-04A method, providing consistency of results and therefore real applicability of the proposed method.

## 2. Material and Methods

### 2.1. Chemicals

All the solutions and colloids were prepared in high pure water (Milli-Q) and only highly pure reagents were used. To wash the glassware, HCl (Carlo Erba) and HNO<sub>3</sub> (Carlo Erba) 3:1 v/v (aqua regia) were used. For the synthesis of the three types of spheroidal AgNPs, AgNO<sub>3</sub> (Panreac), NaBH<sub>4</sub> (Acros Organics) and sodium citrate tribasic dihydrate (Sigma-Aldrich) were used. A solution of 12 % v/v EtOH (Carlo Erba) in water was prepared as the most simplified model system. Wine simulant was prepared according to literature common recipe (Corona et al., 2019, Scafidi et al., 2013) to obtain a 12 % v/v hydro alcoholic solution containing 5 g/l tartaric acid (Sigma-Aldrich). The pH was adjusted to 3 using NaOH 1M (Alfa Aesar) to emulate the typical wine characteristics (Waterhouse, Sacks, & Jeffery, 2016). Potassium metabisulfite (Sigma-Aldrich) was added to reach different concentrations of SO<sub>2</sub> considering their solubilisation yield due to acid/base equilibria. For the official method, the following reagents were used: phosphoric acid 85 % (Honeywell Fluka™), hydrogen peroxide solution (Merck), 0.01 M sodium hydroxide (Scharlau), indicator reagent: Methyl Red (Merck), Methylene Blue (Merck), ethanol 50 % (v/v) 100 ml (VMR).

## 2.2. Synthesis of AgNPs colloids

All glassware used in the synthesis was soaked in aqua regia (HCl:HNO<sub>3</sub> 3:1 v/v), rinsed thoroughly in water and dried with nitrogen prior to use. AgNPs with a nominal diameter of 4 nm, 30 nm and 55 nm were synthesized according to a seeding-growth procedure proposed by Wan et al. (2013). Briefly, 4 nm AgNPs were prepared by adding 20 ml of a 1 % (w/v) citrate solution and 75 ml of water in a round bottom flask and the mixture was heated in an oil bath to 70 °C for 15 min. After that, 1.7 ml of a 1 % (w/v) AgNO<sub>3</sub> solution was introduced in the mixture, followed by the quick addition of 2 ml of a 0.1 % (w/v) freshly prepared ice-cooled NaBH<sub>4</sub> solution. The reaction solution was kept at 70 °C under vigorous stirring for 1 h and cooled down to room temperature. Water was added to bring the volume of the dispersion to 100 ml. The resulting AgNPs were used as starter seeds.

To obtain larger AgNPs, stepwise seeding growth was employed. For the synthesis of AgNPs of 30 nm, 2 ml of a 1 % citrate solution was mixed with 75 ml of water and brought to boiling for 15 min. Then, 10 ml of starter seed solution was added while vigorous mechanical stirring, followed by the addition of 1.7 ml of a 1 % AgNO<sub>3</sub> solution. Vigorously mechanical stirring continued for 1 h while keeping reflux. Then, the next step involved the addition of 2 ml of a 1 % citrate solution to the reaction solution together with 1.7 ml of a 1 % AgNO<sub>3</sub> solution. Reflux with vigorous stirring continued for another one hour. The same operation was then repeated again. After that, the reaction solution was cooled down to room temperature and water was added to bring the volume to 100 ml. For AgNPs of 55 nm, the resulting 30 nm AgNPs were used as seeds. 2 ml of a 1 % citrate solution was mixed with 80 ml of water and brought to 80 °C for 15 min. Next, 10 ml of the seed solution was added while vigorously mechanical stirring, followed by the addition of 1.7 ml of a 1 % AgNO<sub>3</sub> solution. The reaction solution was kept heating at 80 °C under vigorous mechanical stirring for 2 h and cooled down to room temperature. Water was added to bring the volume to 100 ml.

## 2.3 AgNPs size distribution analysis by transmission electron microscopy

The AgNPs images were collected with a Transmission Electron Microscope, TEM, (JEOL JEM 3010-UHR) with a point resolution of 0.17 nm equipped with a thermo-ionic source (monocrystal of LaB<sub>6</sub>). A voltage of 300 kV was used. A drop of AgNPs colloid was deposited on a 3 mm copper grid, previously covered by a perforated carbon thin film, and left to dry in air before being analysed. To measure the AgNPs diameter, at least 200 NPs were analysed for each sample by TEM micrographs with the ImageJ software (Abràmoff, Magalhaes, & Ram, 2004). The specific surface area was calculated dividing the superficial area of one NP (approximating the NPs shape to a sphere) by its mass (considering the Ag density of 10.49 g/cm<sup>3</sup>).

## 2.4. AgNPs characterization by inductively coupled plasma-mass spectrometry

In order to evaluate the total amount of Ag in the samples, a complete mineralization of the nanoparticles was carried out. 0.5 ml of the different AgNPs samples were dissolved using a small amount of hot nitric acid and then diluted 1-10,000. The final percentage of HNO<sub>3</sub> in the solution was 2 % w/w. The final solution was then analysed with an inductively coupled plasma-mass spectrometry ICP-MS in order to quantify the Ag.

ICP-MS analyses were carried out using a Thermo Fisher Scientific ICP-MS ICAP-Qs model, equipped with a quadrupole mass analyser and a flagpole quadrupole collision / reaction cell. The instrument was calibrated with a 2 % HNO<sub>3</sub> standard for Ag, prepared by diluting the reference at 1000 mg/l using <sup>45</sup>Sc, <sup>89</sup>Y, <sup>159</sup>Tb (100 µg/l) as internal standards. The calibration curve was constructed with 6 points and linear correlation coefficient > 0.999. Interference due to polyatomic ions was eliminated by operating the collision cell in He mode with kinetic energy discrimination (He - KED). <sup>107</sup>Ag was used for quantitation. RF power of 1450 W, an argon flow of 15 l/min, an auxiliary argon flow of 1.0 l/min, a nebulized flow of 0.90 l/min and a helium flow in the collision chamber of 5.0 ml/min were used as operating parameters.

## **2.5. AgNPs characterization by UV-vis spectroscopy**

UV-Vis spectra of the different AgNPs colloids were acquired by a UV-Vis spectrophotometer (Hach) in the spectral range 200 - 1100 nm in polystyrene cuvette (10 mm path length). To avoid signal saturation, AgNPs colloids were diluted in water before the analysis as follows: 1:10 for the 4 nm AgNPs; 1:40 for 30 nm and 55 nm AgNPs. For investigating the interaction between AgNPs and SO<sub>2</sub> in different matrices, AgNPs with different size were mixed with SO<sub>2</sub> solutions at 1:1 ratio and further diluted in water to keep the same dilution factors previously described. In the case of the wine samples, the UV-Vis spectra were carried out by mixing 1:1 AgNPs colloids and the wine samples with different SO<sub>2</sub> additions.

## **2.6. Wine samples preparation for SERS analysis**

ISOLUTE® C18 solid-phase extraction cartridges (Biotage, 1 g/6 ml) were used to pre-clean wine samples. The cartridges were activated with 5 ml of MeOH (Carlo Erba) and rinsed with 5 ml of H<sub>2</sub>O. Then, 5 ml of wine was passed through the cartridge at atmospheric pressure. To rinse the cartridge, 5 ml of water was used ending up with a purified sample diluted in a ratio of 1:2. Three white wines (Chardonnay, Grillo and Favorita) and three red wines (Dolcetto, Chianti and Freisa) were bought in a local market and analysed. Each sample was prepared and measured in triplicate. For the SERS quantification, standard additions were made in such a way that the wine sample (already diluted 1:2 after the pre-cleaning in the cartridge) was spiked with a progressively increasing known concentration, i.e. 10 mg/l, 20 mg/l, 30 mg/l, 40 mg/l and 50 mg/l, of SO<sub>2</sub>, but subjected to a low dilution factor. To do this, 1450 µl of pre-cleaned wine sample and 50 µl of concentrated SO<sub>2</sub> solutions with increasing concentration were sequentially added to 1500 µl of AgNPs suspension.

## **2.7. SERS measurements and data analysis**

SERS spectra were collected using a Thermo Fisher Scientific DXR Raman spectrometer (Waltham, USA) equipped with an excitation laser source at 532 nm and a charge-coupled device (CCD) detector. Raman equipment is weekly calibrated through a software-controlled calibration tool which corrects the frequency scale using multiple neon emission lines and, as a control, verifies the multiple polystyrene Raman peaks, while a white light source is used for the CCD calibration intensity. The grating resolution is 5 cm<sup>-1</sup> (the grating density 900 lines/mm) and the uncertainty associated with the intensity is demonstrated to be lower than 5 %

using a polystyrene standard. SERS measurements were performed using an accessory for liquid measurements with a quartz cuvette. The analysed liquid mixtures were composed of AgNPs colloid and the samples, in ratio 1:1. The spectra were collected with a 10 mW laser power, a rectangular aperture of 50  $\mu\text{m}$  in a spectral range from 50  $\text{cm}^{-1}$  to 3400  $\text{cm}^{-1}$ . The acquisition time for each spectrum was 1 second for 50 exposures. Every measurement was repeated at least three times to evaluate the measurement repeatability. The SERS intensity of the initial sample and of each standard addition was then plotted as a function of the concentration. A linear fit was calculated using the weighted total least square (WTLS) regression by CCC software (Malengo & Pennechi, 2013). The concentration of  $\text{SO}_2$  was calculated as the negative extrapolation of the fit for  $y = 0$  and corrected by appropriate dilution factor. The uncertainty associated with the results took into account the concentration contribution (variance on the x) and the repeatability of the SERS measurements contribution (variance on the y). The fit uncertainty was propagated by the Monte Carlo method in accordance with international guidelines (*Evaluation of measurement data – Supplement 1 to the “Guide to the expression of uncertainty in measurement” – Propagation of distributions using a Monte Carlo method*, 2008), using the NIST Uncertainty Machine (Lafarge & Possolo, 2015). The LOD of SERS method was calculated for each tested wine considering the standard deviation of the blank and the slope of the line fitting the experimental data using the equation  $\text{LOD} = 3\text{s}_{\text{dblank}}/b$  (A. Shrivastava, 2011).

## 2.8. OIV-MA-AS323-04A official method

As verification, the OIV-MA-AS323-04A method for the determination of total sulfur dioxide content was also tested with the same samples. 20 ml of wine sample and 5 ml of phosphoric acid were mixed into a 250 ml round-bottom vacuum flask (the flask was labelled with A in the Figure S1 in supplementary information). 3 ml of hydrogen peroxide solution, two drops of the indicator and 0.01 M NaOH solution in order to neutralize this solution, were placed in the bubbler labelled with B.

The wine in the flask A was brought to boiling temperature while an air flux passed through for 15 min. The air flux dragged the  $\text{SO}_2$  liberated gas from the sample to the flask B, where it was oxidized to sulfuric acid by  $\text{H}_2\text{O}_2$ . The formed  $\text{H}_2\text{SO}_4$  was then determined by titration with NaOH 0.01 M.

## 3. Results and Discussion

### 3.1. Characterization of AgNPs colloids

Spheroidal AgNPs with a nominal diameter of 4 nm, 30 nm and 55 nm were synthesized, as reported in paragraph 2.2, and promptly characterized by TEM and UV-Vis measurements in terms of shape, size and plasmon resonance wavelength (Fig. S2). The  $\lambda_{\text{max}}$ , which indicates the wavelength of the characteristic Local Surface Plasmon Resonance (LSPR), increases from 391 nm to 417 nm, showing a red-shift of the LSPR peak as the relative particle size gets bigger (He, Liang, & Peng Peng, 2017; Hong & Li, 2013). The symmetry of the absorption peaks for the 4 nm (TEM diameter  $6 \pm 3$  nm) and 30 nm (TEM diameter  $30 \pm 6$  nm) AgNPs attests a good homogeneity in terms of size distribution and spheroidal shape, which was also confirmed by

TEM analysis. In the case of 55 nm AgNPs (TEM diameter  $53 \pm 7$  nm), instead, the symmetry of the LSPR peak was not preserved, showing a main peak at 417 nm, together with a small shoulder around 370 nm, which could be associated both to new nucleation phenomena and to asymmetric particles growth during the seeding-growth synthesis. In this case, the presence of a population of non-spherical NPs was revealed by TEM analysis as already commented by Wan et al. (2013) in their contribution. Based on both TEM and ICP measurements, the concentration of AgNPs with different sizes and their specific surface area were calculated, providing that the smallest NPs contain the lowest amount of Ag atoms, but they show a specific surface area 5 times higher than the 30 nm AgNPs, and 9 times higher than the 55 nm AgNPs (Table S1).

### 3.2. Interaction of AgNPs with SO<sub>2</sub> in EtOH/H<sub>2</sub>O environment

Several studies already proposed metallic NPs as useful substrates for additives and contaminants detection in food and beverages, where a strong chemical interaction between the colloids and the analyte occurred (Kang, Hwang, Lee, & Lee, 2002). This binding affinity normally leads to the agglomeration of the NPs generating clustered SERS hot spots which are responsible for a huge enhancement of Raman signals (Giovannozzi et al., 2014). In order to investigate the reactivity of differently sized NPs and to select the best AgNPs for the specific application *in liquid* measurement of SO<sub>2</sub> in wine, the chemical interaction of AgNPs with sulfur-containing species was initially studied performing AgNPs agglomeration tests in suspension (Fig. 1). A preliminary investigation of the reactivity was conducted by acquiring UV-Vis and SERS spectra in EtOH/H<sub>2</sub>O solutions. In Figure 1a, the UV-Vis spectra of each type of AgNPs (solid lines) and of the same AgNPs mixed with 100 mg/l of SO<sub>2</sub> (dash lines) are reported. The SERS spectra of the three AgNPs with 5 mg/l of SO<sub>2</sub> are shown in Fig. 1b. This concentration was chosen to evaluate the sensitivity of the method in the lower part of the concentration range of interest for this study. As a control test, Raman spectra, without AgNPs, of concentrated SO<sub>2</sub> solutions (100 mg/l) were also measured, confirming that the sensitivity of Raman technique is too low to reveal the typical SO<sub>2</sub> bands in absence of the enhancement effect. Only ethanol peaks were revealed by normal Raman measurements, as shown in the black spectrum in Fig. 1b.

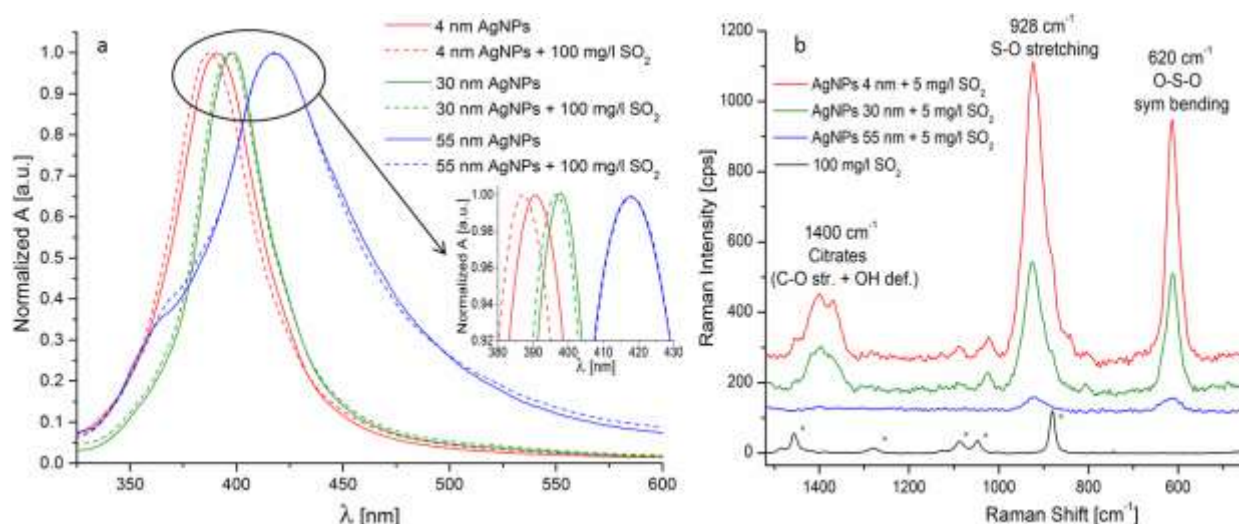


Figure 1. a) Normalized UV-Vis spectra in EtOH/H<sub>2</sub>O of the diluted AgNPs colloids with different sizes (4 nm, 30 nm, 55 nm, solid lines) and of the AgNPs colloids mixed with 100 mg/l of SO<sub>2</sub> solutions (dash lines); b) SERS spectra of AgNPs of different sizes (4 nm, 30 nm, 55 nm) with the addition of 5 mg/l of SO<sub>2</sub> in EtOH/H<sub>2</sub>O, and Raman spectrum of 100 mg/l of SO<sub>2</sub> in EtOH/H<sub>2</sub>O without AgNPs. The peaks marked with \* are related to EtOH.

From the spectra obtained by UV-vis and Raman, it emerges that the behaviour of AgNPs with SO<sub>2</sub> differs depending on the size of the NPs. In the case of 55 nm AgNPs, the addition of SO<sub>2</sub> does not cause a significant variation in the UV-Vis spectrum. On the contrary, 4 nm and 30 nm AgNPs show a blue-shift of the LSPR after the addition of 100 mg/l of SO<sub>2</sub>. In particular, for 4 nm AgNPs, the shift of the LSPR peak is more evident (a shift of 4 nm was registered). In Fig. S3, the progressive blue shift obtained by increasing the concentration of SO<sub>2</sub> in solution from 0 mg/l to 100 mg/l is shown. This experimental evidence could be explained by considering the binding of sulfur species on the Ag surface, which substitute the shell of citrate ions, here used as reductant and stabilizing agent during the AgNPs synthesis. The presence of sulfur species on the Ag surface provokes a changing of the surface chemistry and a decrease of the global diameter of dispersed NP (considering both the Ag spheroid and the surrounding shell), with a consequent blue shift of the LSPR peak. In agreement with these results, the peaks associated with the vibrational modes of SO<sub>2</sub> are visible in the SERS spectra (Fig. 2b). Indeed, thanks to the chemical affinity between S and Ag, SO<sub>2</sub> bound to the surface of AgNPs provides two intense and quite broad bands at 928 cm<sup>-1</sup> and 620 cm<sup>-1</sup> due to S-O stretching (sym. + asym.) and O-S-O sym. bending modes, respectively (Chen et al., 2016; Deng et al., 2015). The band at 928 cm<sup>-1</sup> is partially overlapped with the EtOH peak at 900 cm<sup>-1</sup>, which is responsible for a left shoulder in case of a low intensity of the S-O stretching band. Testing differently sized AgNPs, the highest SERS intensity of the SO<sub>2</sub> modes was obtained with the 4 nm AgNPs, while the S-O bands were barely identifiable using the 55 nm AgNPs. The higher SERS intensity obtained for 4 nm AgNPs is probably due to the higher concentration of small AgNPs, even though the total amount of Ag in suspension was lower than in the other tested AgNPs suspensions (see Table S1). This results in a greater specific surface area for small NPs, which is probably responsible for a higher reactivity and a higher enhancement effect. This observation is coherent with the UV-Vis findings, where the interaction of SO<sub>2</sub> and AgNPs colloids was maximized for the smallest NPs. As a result, the 4 nm AgNPs were selected for subsequent experiments.

### 3.3. Interaction of AgNPs and SO<sub>2</sub> in wine simulant environment

The wine simulant at pH = 3 was used to investigate the interaction of AgNPs and SO<sub>2</sub> in a model system similar to the matrix of interest, i.e. the wine. A relevant agglomeration of AgNPs was noticed when AgNPs were mixed with the wine simulant in absence of sulfites (the solution colour changed from yellow to red). As Fig. 2a shows, the main AgNPs absorption peak decreases and a shoulder around 530 nm appears, attributable to AgNPs agglomerates. When the AgNPs were added to wine

simulant containing sulfites, the colour turned to dark green and the corresponding absorption peak broadened and became significantly less intense. The pH influenced the surface charge on AgNPs on the base of the  $pK_a$  values of the three carboxylic groups of the citrate ions ( $pK_a = 3.13, 4.76$  and  $6.34$ ). At  $pH = 3$ , the carboxylic groups are completely protonated reducing the repulsive forces among AgNPs and promoting agglomeration. Moreover, the presence of sulfites provoked an interaction due to a chemical affinity of S-containing species with the AgNPs surface and a stronger agglomeration of AgNPs, that can be easily monitored by UV-Vis absorption measurements (Fig. 2a). This strong agglomeration of AgNPs was responsible for the creation of SERS hot-spots in suspension and allowed the enhancement of  $SO_2$  signals. Comparing the SERS spectra of  $SO_2$  in the hydro alcoholic environment and in wine simulant, an intensification of the signals of about 80 % is observable in wine simulant (Fig. 2b). In EtOH/ $H_2O$  environment, the band at  $928\text{ cm}^{-1}$  of  $SO_2$  is flanked by an EtOH peak, which is not visible when  $SO_2$  band signals are more intense. In Fig. 2b, another band is visible at  $1400\text{ cm}^{-1}$  in the highly enhanced spectrum. This peak is probably due to citrates (stretching CO + deformation OH), which remain bounded to the NPs surface. Solutions at different  $SO_2$  concentrations between 0 mg/l and 100 mg/l were mixed with an equal volume of 4 nm AgNPs suspension and directly analysed by SERS in liquid phase.

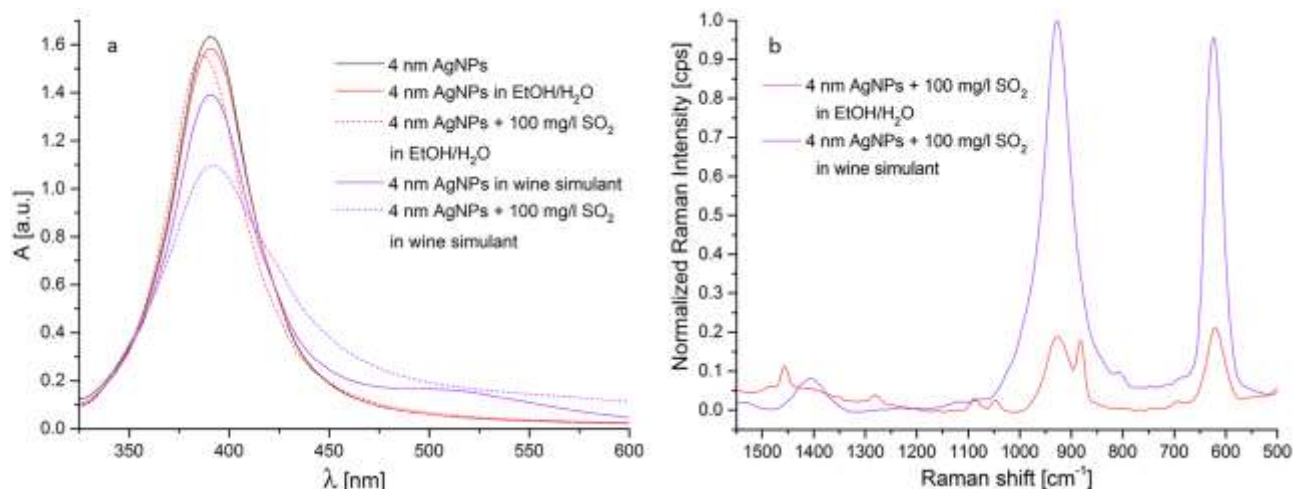


Figure 2. a) UV-Vis spectra of 4 nm AgNPs colloid and of 4 nm AgNPs with the addition of 100 mg/l of  $SO_2$  in the different solutions (water, EtOH/ $H_2O$  and wine simulant); b) Normalized SERS spectra of 4 nm AgNPs with the addition of 100 mg/l of  $SO_2$  in EtOH/ $H_2O$  and in wine simulant.

Average spectra of three measurement repetitions are reported in Fig. 3. An increasing intensity trend is observed for both  $SO_2$  bands at  $928\text{ cm}^{-1}$  and  $620\text{ cm}^{-1}$  for progressively more concentrated standards. The experimental data can be fitted with a Langmuir function typical for adsorption-desorption phenomena (Kinniburgh, 1986), with a correlation factor of 0.94 (Fig. 3b). It is noteworthy

that the citrate peak at  $1400\text{ cm}^{-1}$  shows an opposite trend compared to  $\text{SO}_2$  peaks. This could be explained as a progressive substitution of citrates with  $\text{SO}_2$  on the NPs surface. It is also interesting to note that the exponential decay of the SERS peak of citrates reached a plateau beyond the  $\text{SO}_2$  concentration of  $25\text{ mg/l}$  and that a further blue shift of the maximum of the UV-Vis absorption peak of  $4\text{ nm}$  AgNPs is not observed beyond this concentration of  $\text{SO}_2$  (Fig. S3). This evidence could indicate that, at the  $\text{SO}_2$  concentration of  $25\text{ mg/l}$ , an equilibrium for citrates substitution with  $\text{SO}_2$  on the  $4\text{ nm}$  AgNPs surface was obtained. Nevertheless, as the  $\text{SO}_2$  concentration increased, other  $\text{SO}_2$  molecules were adsorbed on the  $4\text{ nm}$  AgNPs free surface, as evinced by the rise of the SERS peaks intensity. This could be explained by the greater steric hindrance of the removed citrates compared to the  $\text{SO}_2$  one on  $4\text{ nm}$  AgNPs surface. In Fig. S4, the three peaks of Fig. 3a are reported separately. In particular, Fig. S4c shows the peak at  $620\text{ cm}^{-1}$ , which slightly shifted toward higher frequency as the  $\text{SO}_2$  concentration increases over  $25\text{ mg/l}$  of  $\text{SO}_2$ , that can be ascribed to adsorbate-adsorbate interactions on AgNPs surface (Coluccia, Baricco, Marchese, Martra, & Zecchina, 1993).

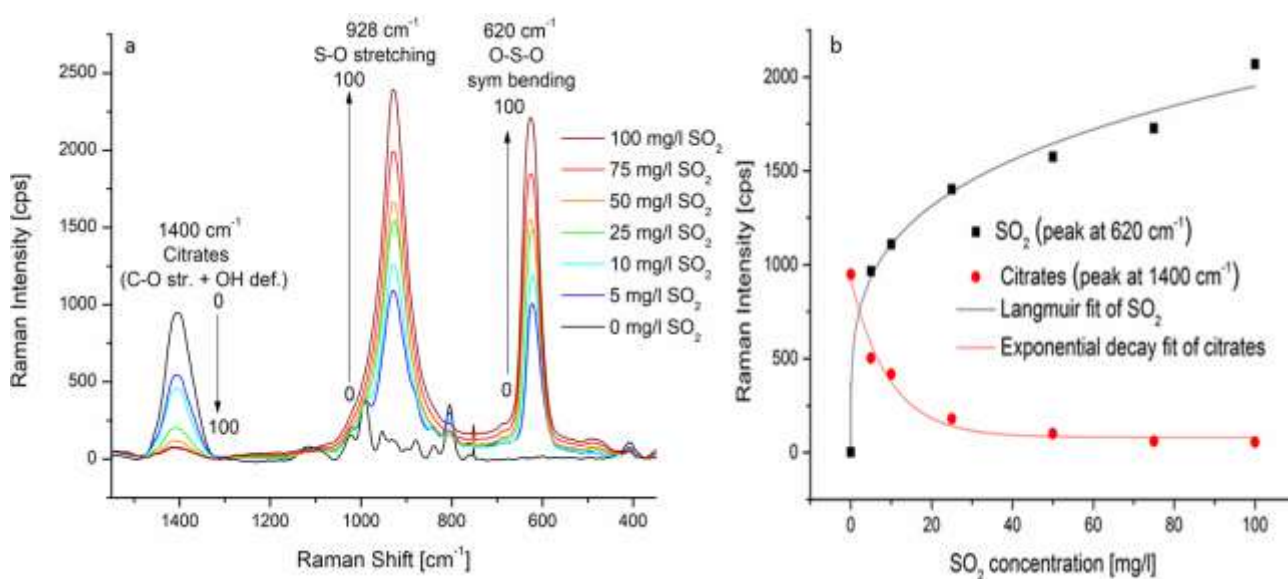


Figure 3. a) SERS intensity trend from  $0\text{ mg/l}$  to  $100\text{ mg/l}$  of  $\text{SO}_2$  with  $4\text{ nm}$  AgNPs in wine simulant. b) Curve fits of the Raman intensities of the peak at  $620\text{ cm}^{-1}$  for  $\text{SO}_2$  (Langmuir fit) and of the peak at  $1400\text{ cm}^{-1}$  for citrates (exponential decay fit).

### 3.4. $\text{SO}_2$ quantification in wine samples and comparison with the official method

When the quantification of  $\text{SO}_2$  is performed in wine samples, the presence of numerous chemical species that are able to interact with AgNPs cannot be neglected. AgNPs agglomerate severely when mixed with wine, showing a drastic colour change from yellow to dark purple with the appearance of

a new band ascribed to AgNPs aggregates around 570 nm (the UV-vis spectra are shown in Fig. S5). Typical SO<sub>2</sub> peaks are clearly observed in the SERS spectra of wine samples, however a high variability of the SERS response was noticed in the analysis of different types of wine. In particular, some spectral features such as the baseline, the noise level and the shape of the peaks were mainly influenced by the ensemble of molecular species and by the pH of different types of wine. Therefore, reverse SPE purification step was performed. C18 SPE for wine samples pretreatment is widely used in literature, in particular Corona, Squadrito, Vento, Tirelli, and Di Stefano (2015) reports the use of C18 as a purification method to completely remove sulfites for an accurate determination of polyphenols. Xiong, Wang, Li, Fang, and Duan (2018), instead, reports the use of reverse SPE to eliminate the interference of organic impurities and colored materials in red wines before the accurate quantification of sulfites by ionic chromatography. In this study SPE is exploited as unspecific purification step. Interfering compounds as polyphenols, terpenes, planar organics etc. are trapped in the cartridge thanks to the attractive forces between organics and the functional groups on the silica sorbent, as previously demonstrated in literature (Dziadas & Jelen, 2010; Picron, Herman, Van Hoeck, & Goscinny, 2018). A recovery of sulfites after the SPE close to 100 %, confirmed that no SO<sub>2</sub> losses occurred during sample pretreatment, but colored organics are not quantitatively removed (Table S3).

However, wine variability in terms of composition of organics and pH prevented the application for all types of wine samples of a unique calibration curve based on the standards prepared in wine simulant. Indeed, at the slightly different pH values of different wines, the agglomeration process of AgNPs could be more or less severe. This produces a different concentration of SERS hotspots and generates differences in terms of SERS intensity of the analyte signals. Moreover, the pH also influences the forms of sulfur species in water, determining different interaction with AgNPs and consequently different SERS response. For these reasons, a unique calibration curve cannot be used for different wine samples. The standard additions strategy was chosen to quantify the SO<sub>2</sub> content in wine samples, overcoming the peculiar matrix effect of different wines.

As an example, the SERS spectra of Dolcetto red wine with the progressive additions of SO<sub>2</sub> are reported in Fig. 4a. In Fig. 4b, the plot of the SERS intensity at 620 cm<sup>-1</sup> as a function of the added SO<sub>2</sub> amount used to extrapolate the concentration of SO<sub>2</sub> initially present in the Dolcetto red wine is shown. Considering that the slope of the linear fit changed depending on the type of wine, it was not possible to provide a general LOD for the technique. The LOD was calculated for all tested wines and the results are shown in Table 1, with the best values obtained for Grillo and Favorita white wines which have a LOD of 0.6 mg/l. All the obtained values are adequate with respect to the field of application, where low limits are over 100 mg/l.

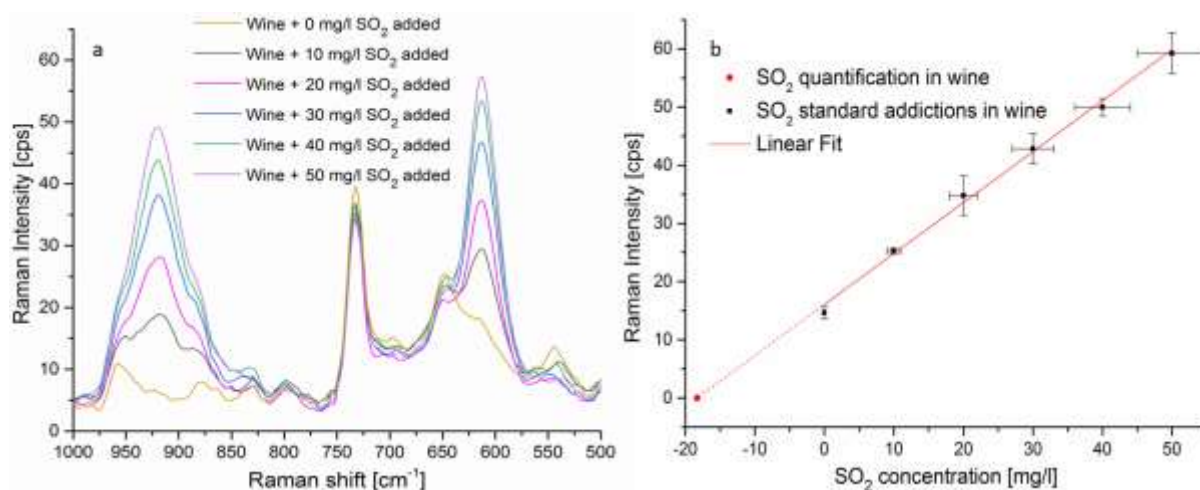


Figure 4. a) SERS spectra of 4 nm AgNPs colloid with different addition of SO<sub>2</sub> in pre-cleaned Dolcetto red wine; b) Fit of the Raman intensity of the peaks at 620 cm<sup>-1</sup> and extrapolation of the SO<sub>2</sub> concentration value in wine approximately diluted at 1:4.

Table 1 reports the results of SO<sub>2</sub> content in white and red wines achieved with the proposed *in liquid* SERS method compared with the values obtained using the official OIV method, here used as a reference, and the percentage error, which is lower than 5 % in most of cases. A good agreement in the quantification of the SO<sub>2</sub> content was achieved, providing the validation of this innovative method.

**Table 1**

Quantification of SO<sub>2</sub> in real wine samples by the in liquid SERS method and by the official method.

Wine	SERS LOD [mg/l]	SO <sub>2</sub> by SERS* [mg/l]	St. dev. [mg/l]	SO <sub>2</sub> by OIV method* [mg/l]	St. dev. [mg/l]	Error %
Chardonnay	9.6	61.4	1	64	3.7	4.06
Grillo	0.6	124.5	9.2	111.4	2.6	11.8
Favorita	0.6	72.7	3.9	78	2.5	6.79
Dolcetto	1.5	71.1	3.2	70.4	1.9	0.99
Chianti	3.9	101.5	9.3	97.9	2	3.68
Freisa	1.1	82.2	5	81.1	2.6	1.36

## 4. Conclusions

The interaction of AgNPs with different size with the SO<sub>2</sub> in hydro alcoholic solutions, in wine simulant and in wine samples was studied. The UV-Vis and SERS spectra showed that the greatest interaction between SO<sub>2</sub> and NPs was obtained with the 4 nm AgNPs due to their greater specific surface. For this reason, the 4 nm AgNPs were selected for quantitative analysis in wine samples. A direct proportionality between the SO<sub>2</sub> concentration in the samples and the SERS intensity of the two SO<sub>2</sub> peaks was obtained in the range 0 - 100 mg/l in wine simulant. In particular, the data of SERS intensities of SO<sub>2</sub> peaks were fitted with a Langmuir function (correlation factor = 0.94), characteristic of adsorption-desorption phenomena. The proportional trend was conserved also in wine samples, even though the matrix effect strongly affected the spectra, preventing the use of a unique calibration curve. In this study, three white wines (Chardonnay, Grillo and Favorita) and three red wines (Dolcetto, Chianti and Freisa) were analysed by SERS, and quantitative results were obtained by standard addition method. The results achieved by SERS were consistent with those obtained by the official OIV method, ensuring the validity of this new *in liquid* SERS methodology for the quantification of total SO<sub>2</sub> content in wine samples. Moreover, SERS technique equipped with a portable Raman spectrometer, which can provide rapid and sensitive detection for *on-site* testing, paves the way for interesting winery applications.

### **Acknowledgements**

This work was supported by Progetto IMPreSA (POR FESR 2014/20 - Asse I, Azione I.1.a.1.5 INFRA-P Sostegno alle infrastrutture di ricerca considerate critiche/cruciali per i sistemi regionali) from Regione Piemonte.

### **Declaration of interests**

The authors declare that they have no known competing financial interests or personal relationships that could have appeared to influence the work reported in this paper.

### **Author contribution section**

LM, AG, IC designed the experiments; LB, IC, LM, FP, AA performed the experiments; LM, IC, LB, AG, FP analysed the data, LM, IC, FD wrote the manuscript. AR, MP provided founding and supervised the project. The manuscript was written through contributions of all authors. All authors gave approval to the final version of the manuscript.

### **Appendix A. Supplementary data**

Supplementary data to this article can be found online at <https://doi.org/10.1016/j.foodchem.2020.127009>.

## References

- A. Shrivastava, V. B. G. A. (2011). Methods for the determination of limit of detection and limit of quantitation of the analytical methods. *Chronicles of Young Scientists*, 2(1), 21. <https://doi.org/10.4103/2229-5186.79345>.
- Azevedo, C. M. N., Araki, K., Toma, H. E., & Angnes, L. (1999). Determination of sulfur dioxide in wines by gas-diffusion flow injection analysis utilizing modified electrodes with electrostatically assembled films of tetra-ruthenated porphyrin. *ANALYTICA CHIMICA ACTA*, 387(2), 175–180. [https://doi.org/10.1016/S0003-2670\(99\)00060-4](https://doi.org/10.1016/S0003-2670(99)00060-4).
- Cara, E., Mandrile, L., Lupi, F. F., Giovannozzi, A. M., Dialameh, M., Portesi, C., ... Boarino, L. (2018). Influence of the long-range ordering of gold-coated Si nanowires on SERS. *SCIENTIFIC REPORTS*, 8. <https://doi.org/10.1038/s41598-018-29641-x>.
- Cardwell, T. J., Cattrall, R. W., Chen, G. N., Scollary, G. R., & Hamilton, I. C. (1991). Determination of free sulfur-dioxide in red wine by alternating-current voltammetry. *ANALYST*, 116(3), 253–256. <https://doi.org/10.1039/an9911600253>.
- Chen, M., Yang, H., Rong, L., & Chen, X. (2016). A gas-diffusion microfluidic paper-based analytical device ( $\mu$  PAD) coupled with portable surface-enhanced Raman scattering (SERS): Facile determination of sulphite in wines. *ANALYST*, 141(19), 5511–5519. <https://doi.org/10.1039/c6an00788k>.
- Coluccia, S., Baricco, M., Marchese, L., Martra, G., & Zecchina, A. (1993). Surface-morphology and reactivity towards CO of MGO particles – FTIR and HRTEM studies. *SPECTROCHIMICA ACTA PART A-MOLECULAR AND BIOMOLECULAR SPECTROSCOPY*, 49(9), 1289–1298. [https://doi.org/10.1016/0584-8539\(93\)80036-A](https://doi.org/10.1016/0584-8539(93)80036-A).
- Corona, O., Squadrito, M., & Tirelli, A. (2019). Factors affecting the spectrophotometric

quantification of flavonoids in wine. *ITALIAN JOURNAL OF FOOD SCIENCE*, 31(3), 459–469.

Corona, O., Squadrito, M., Vento, G., Tirelli, A., & Di Stefano, R. (2015). Over-evaluation of total flavonoids in grape skin extracts containing sulphur dioxide. *FOOD CHEMISTRY*, 172, 537–542. <https://doi.org/10.1016/j.foodchem.2014.09.125>

Craig, A. P., Franca, A. S., & Irudayaraj, J. (2013). Surface-Enhanced Raman Spectroscopy applied to food safety. In M. P. Doyle, & T. R. Klaenhammer (Eds.), *ANNUAL REVIEW OF FOOD SCIENCE AND TECHNOLOGY, VOL 4* (pp. 369–380). <https://doi.org/10.1146/annurev-food-022811-101227>

Dalla Marta, S., Novara, C., Giorgis, F., Bonifacio, A., & Sergio, V. (2017). Optimization and characterization of paper-made surface enhanced Raman scattering (SERS) substrates with Au and Ag NPs for quantitative analysis. *MATERIALS*, 10(12). <https://doi.org/10.3390/ma10121365>.

Deng, Z., Chen, X., Wang, Y., Fang, E., Zhang, Z., & Chen, X. (2015). Headspace thin-film microextraction coupled with surface-enhanced Raman scattering as a facile method for reproducible and specific detection of sulfur dioxide in wine. *ANALYTICAL CHEMISTRY*, 87(1, SI), 633–640. <https://doi.org/10.1021/ac503341g>.

Dziadas, M., & Jelen, H. H. (2010). Analysis of terpenes in white wines using SPE-SPME-GC/MS approach. *ANALYTICA CHIMICA ACTA*, 677(1, SI), 43–49. <https://doi.org/10.1016/j.aca.2010.06.035>.

E. Li-Chan, J.M. Chalmers, P. R. G. (2010). *Applications of Vibrational Spectroscopy in Food Science* (Jhon Wiley& Sons, ed.).

*Evaluation of measurement data – Supplement 1 to the “Guide to the expression of uncertainty in*

measurement” – *Propagation of distributions using a Monte Carlo method*. (2008). Retrieved from [https://www.bipm.org/utils/common/documents/jcgm/JCGM\\_101\\_2008\\_E.pdf](https://www.bipm.org/utils/common/documents/jcgm/JCGM_101_2008_E.pdf).

Gastaminza, G., Quirce, S., Torres, M., Tabar, A., Echechipia, S., Munoz, D., & Decorres, L. F. (1995). Pickled onion-induced asthma – A model of sulfite-sensitive asthma. *CLINICAL AND EXPERIMENTAL ALLERGY*, 25(8), 698–703. <https://doi.org/10.1111/j.1365-2222.1995.tb00006.x>.

Giovannozzi, A. M., Rolle, F., Segal, M., Abete, M. C., Marchis, D., & Rossi, A. M. (2014). Rapid and sensitive detection of melamine in milk with gold nanoparticles by Surface Enhanced Raman Scattering. *FOOD CHEMISTRY*, 159, 250–256. <https://doi.org/10.1016/j.foodchem.2014.03.013>.

Hong, S., & Li, X. (2013). Optimal size of gold nanoparticles for surface-enhanced Raman spectroscopy under different conditions. *JOURNAL OF NANOMATERIALS*. <https://doi.org/10.1155/2013/790323>.

Huang, Y. M., Zhang, C., Zhang, X. R., & Zhang, Z. J. (1999). Chemiluminescence of sulfite based on auto-oxidation sensitized by rhodamine 6G. *ANALYTICA CHIMICA ACTA*, 391(1), 95–100. [https://doi.org/10.1016/S0003-2670\(99\)00179-8](https://doi.org/10.1016/S0003-2670(99)00179-8).

Kang, J. S., Hwang, S. Y., Lee, C. J., & Lee, M. S. (2002). SERS of dithiocarbamate pesticides adsorbed on silver surface; Thiram. *BULLETIN OF THE KOREAN CHEMICAL SOCIETY*, 23(11), 1604–1610.

Kinniburgh, D. G. (1986). General purpose adsorption isotherms. *Environmental Science & Technology*, 20(9), 895–904.

Koch, M., Koeppen, R., Siegel, D., Witt, A., & Nehls, I. (2010). Determination of total sulfite in wine by ion chromatography after in-sample oxidation. *JOURNAL OF AGRICULTURAL AND*

*FOOD CHEMISTRY*, 58(17), 9463–9467. <https://doi.org/10.1021/jf102086x>.

Lafarge, T. & Possolo, A. (2015). The NIST uncertainty machine. *NCSLI Measure*, 10(3), 20–27. <https://doi.org/doi.org/10.1080/19315775.2015.11721732>.

Liu, Z., Cheng, L., Zhang, L., Jing, C., Shi, X., Yang, Z., ... Fang, J. (2014). Large-area fabrication of highly reproducible surface enhanced Raman substrate via a facile double sided tape-assisted transfer approach using hollow Au-Ag alloy nanourchins. *NANOSCALE*, 6(5), 2567–2572. <https://doi.org/10.1039/c3nr05840a>.

Malengo, A., & Pennechi, F. (2013). A weighted total least-squares algorithm for any fitting model with correlated variables. *METROLOGIA*, 50(6), 654–662. <https://doi.org/10.1088/0026-1394/50/6/654>.

Mandrile, L., Giovannozzi, A. M., Durbiano, F., Martra, G., & Rossi, A. M. (2018). Rapid and sensitive detection of pyrimethanil residues on pome fruits by Surface Enhanced Raman Scattering. *FOOD CHEMISTRY*, 244, 16–24. <https://doi.org/10.1016/j.foodchem.2017.10.003>.

Abràmoff, M. D., Magalhaes, P. J., & Ram, S. J. (2004). Image processing with ImageJ. *Biophotonics International*, 11(7), 36–42.

Monro, T. M., Moore, R. L., Nguyen, M.-C., Ebendorff-Heidepriem, H., Skouroumounis, G. K., Elsey, G. M., & Taylor, D. K. (2012). Sensing free sulfur dioxide in wine. *SENSORS*, 12(8), 10759–10773. <https://doi.org/10.3390/s120810759>.

Oliveira, S. M., Lopes, T. I. M. S., Toth, I. V., & Rangel, A. O. S. S. (2009). Development of a gas diffusion multicommutated flow injection system for the determination of sulfur dioxide in wines, comparing malachite green and pararosaniline chemistries. *JOURNAL OF AGRICULTURAL AND FOOD CHEMISTRY*, 57(9), 3415–3422. <https://doi.org/10.1021/jf803639n>.

Ribéreau-Gayon, P., Dubordieu, D., Donèche, B., & Lonvaud, A. (2007). *Handbook of oenology: the*

*microbiology of wine and vinification.*

- Pang, S., Yang, T., & He, L. (2016). Review of surface enhanced Raman spectroscopic (SERS) detection of synthetic chemical pesticides. *TRAC-TRENDS IN ANALYTICAL CHEMISTRY*, 85(A, SI), 73–82. <https://doi.org/10.1016/j.trac.2016.06.017>.
- Picron, J.-F., Herman, M., Van Hoeck, E., & Gosciny, S. (2018). Analytical strategies for the determination of pyrrolizidine alkaloids in plant based food and examination of the transfer rate during the infusion process. *FOOD CHEMISTRY*, 266, 514–523. <https://doi.org/10.1016/j.foodchem.2018.06.055>.
- Prieto, A. M. G., Pavon, J. L. P., & Cordero, B. M. (1994). Gas-diffusion and micellar catalysis in the flow-injection determination of sulfite. *ANALYST*, 119(11), 2447–2452. <https://doi.org/10.1039/an9941902447>.
- He, R. X., Liang, R., & Peng Peng, Y. N. Z. (2017). Effect of the size of silver nanoparticles on SERS signal enhancement. *Journal of Nanoparticle Research*, 19(8), 267.
- Scafidi, P., Pisciotta, A., Patti, D., Tamborra, P., Di Lorenzo, R., & Barbagallo, M. G. (2013). Effect of artificial shading on the tannin accumulation and aromatic composition of the Grillo cultivar (*Vitis vinifera* L.). *BMC PLANT BIOLOGY*, 13. <https://doi.org/10.1186/1471-2229-13-175>.
- Schluecker, S. (2014). Surface-enhanced Raman spectroscopy: Concepts and chemical applications. *ANGEWANDTE CHEMIE-INTERNATIONAL EDITION*, 53(19), 4756–4795. <https://doi.org/10.1002/anie.201205748>.
- Segundo, M. A., & Rangel, A. (2001). A gas diffusion sequential injection system for the determination of sulphur dioxide in wines. *ANALYTICA CHIMICA ACTA*, 427(2), 279–286. [https://doi.org/10.1016/S0003-2670\(00\)01197-1](https://doi.org/10.1016/S0003-2670(00)01197-1).
- Smith, V. J. (1987). Determination of sulfite using a sulfite oxidase enzyme electrode. *ANALYTICAL*

*CHEMISTRY*, 59(18), 2256–2259. <https://doi.org/10.1021/ac00145a010>.

Virga, A., Rivolo, P., Descrovi, E., Chiolerio, A., Digregorio, G., Frascella, F., ... Giorgis, F. (2012).

SERS active Ag nanoparticles in mesoporous silicon: Detection of organic molecules and peptide-antibody assays. *JOURNAL OF RAMAN SPECTROSCOPY*, 43(6), 730–736. <https://doi.org/10.1002/jrs.3086>.

Vo-Dinh, T. (1998). Surface-enhanced Raman spectroscopy using metallic nanostructures. *TRAC-TRENDS IN ANALYTICAL CHEMISTRY*, 17(8–9), 557–582. [https://doi.org/10.1016/S0165-9936\(98\)00069-7](https://doi.org/10.1016/S0165-9936(98)00069-7).

Wan, Y., Guo, Z., Jiang, X., Fang, K., Lu, X., Zhang, Y., & Gu, N. (2013). Quasi-spherical silver nanoparticles: Aqueous synthesis and size control by the seed-mediated Lee-Meisel method. *JOURNAL OF COLLOID AND INTERFACE SCIENCE*, 394, 263–268. <https://doi.org/10.1016/j.jcis.2012.12.037>.

Waterhouse, A. L., Sacks, G. L., & Jeffery, D. W. (2016). *Understanding wine chemistry*. John Wiley & Sons.

Xiong, Y., Wang, Q., Li, X., Fang, S., & Duan, M. (2018). Total sulfur dioxide determination in red wine by suppressed ion chromatography with in-sample oxidation and SPE. *CHROMATOGRAPHIA*, 81(7), 1003–1011. <https://doi.org/10.1007/s10337-018-3538-9>.

Yang, X. F., Guo, X. Q., & Zhao, Y. B. (2002). Novel spectrofluorimetric method for the determination of sulfite with rhodamine B hydrazide in a micellar medium. *ANALYTICA CHIMICA ACTA*, 456(1), 121–128. [https://doi.org/10.1016/S0003-2670\(02\)00005-3](https://doi.org/10.1016/S0003-2670(02)00005-3).